ELSEVIER

Journal of Nuclear Materials 283–287 (2000) 344–348

journal of nuclear materials

www.elsevier.nl/locate/jnucmat

Microstructural examination of V–(3–6%)Cr–(3–5%)Ti irradiated in the ATR-A1 experiment

D.S. Gelles *

Pacific Northwest National Laboratory, MS P8-15, P.O. Box 999, Richland, WA 99352, USA

Abstract

Microstructural examination results are reported for four heats of V–(3–6%)Cr–(3–5%)Ti irradiated in the ATR-A1 experiment to ~4 dpa at 200°C and 300°C to provide an understanding of the microstructural evolution that may be associated with degradation of mechanical properties. Fine precipitates were observed in high density intermixed with small defect clusters for all conditions examined following the irradiation. The irradiation-induced precipitation does not appear to be affected by preirradiation heat treatment or composition.

1. Introduction

Vanadium-based alloys are being developed for application as a first-wall material for magnetic fusion power system. It has been shown that alloys of composition V–(4–5%)Cr–(4–5%)Ti have very promising physical and mechanical properties [1]. Susceptibility of the alloy class to loss of work-hardening capability following irradiation at low temperatures under fusion-relevant conditions is considered to be a major factor in governing the minimum operating temperature of magnetic fusion devices.

Recent irradiation experiments at <430°C have shown that the loss of work-hardening capability and uniform elongation of V–4Cr–4Ti vary from heat to heat [2]. The present effort is a continuation of the effort to provide an understanding of the microstructural evolution in these alloys under irradiation with an expansion of the composition range to V–(3–6%)Cr–(3–5%)Ti by examination of specimens irradiated at low temperatures in the recent ATR-A1 experiment along with corresponding mechanical properties of specimens [3,4].

2. Experimental procedure

Specimens in the form of microscopy disks 3 mm in diameter were included in the ATR-A1 test. Companion miniature tensile specimens were also irradiated providing the opportunity for comparison with shear punch and tensile response [4] at a later date. Twelve specimen conditions were selected for examination comprising four heats of material irradiated side-by-side at two irradiation temperatures with corresponding unirradiated control specimens. The compositions of the heats [5,6] and the specimen conditions examined are shown in Table 1. Compositions covered the range V–(3–6%)Cr–(3–5%)Ti based on the availability of two heats recently prepared by ORNL [3]. All were heat treated at 1000°C for 1 or 2 h under vacuum (<10^{-7} Torr) at ANL.

Specimens were irradiated in ATR-A1 subcapsules AS5 and AS11 [7]. Temperatures and fluences have been estimated for these subcapsules as 284–300°C to 4.1 dpa and 198–212°C to 3.0 dpa, respectively [5], but will be referred to as 300°C to 4 dpa and 200°C to 3 dpa in subsequent text. Specimen preparation and examination involved standard procedures. All images were computer processed and printed from scanned negative information.

3. Results

3.1. Preirradiation microstructures

The purpose of this work was to provide information on effects of radiation on microstructure in order to provide interpretation of mechanical properties response. As a result, emphasis was placed on examination

* Corresponding author. Tel.: +1-509 376 3141; fax: +1-509 376 0418.

E-mail address: ds_gelles@pnl.gov (D.S. Gelles).

0022-3115/00/$ - see front matter
PII: S0022-3115(00)00309-3

Table 1
Conditions of specimens examined by TEM

Specimen ID	Composition wt% [minor elements appm]	Heat #	Heat treatment	Temperature (°C)	Dose (dpa)
P8	V–3.8Cr–3.9Ti [O: 310,	832665,	1000°C/1 h	NA[a]	0
P837	N: 85, C: 80, Si: 783]	BL-71		198–212	3.0
P811, P832				284–300	4.1
P7	V–5.0Cr–5.0Ti [O: 380,	T87,	1000°C/1 h	NA	0
P706	N: 90, C: 110, Si: 550]	BL-72		198–212	3.0
P710				284–300	4.1
P1	V–2.84Cr–3.02Ti [O: 230,	T91	1000°C/2 h	NA	0
P113	N: 62, C: 120, Si: 940]			198–212	3.0
P107, P123				284–300	4.1
P2	V–5.97Cr–2.94Ti [O: 280,	T92	1000°C/2 h	NA	0
P224	N: 95, C: 105, Si: 950]			198–212	3.0
P215				284–300	4.1

[a] NA: not applicable.

of irradiated specimens. However, sufficient information was obtained to provide some comparison of the preirradiation microstructures for all the four heats. All preirradiation microstructures appeared similar consisting, in general, of large equiaxed grains with large Ti,V(O,C,N) precipitate particles non-uniformly distributed [8]. The particles observed were as large as 500 nm in heats 832665 and T87, but were generally 200–300 nm with many smaller particles. However, due to the non-uniform distribution, it is difficult to compare precipitate volume fraction from heat to heat based on electron microscopy. Grain boundaries were often distorted in the vicinity of such particles and many examples could be found where small grains were distributed amongst the larger grains, often where triple points would normally be found. In heats T87 and T92, areas were found where re-crystallization had not occurred retaining a relaxed subgrain structure, but the volume fraction was very low. This may be an indication that higher chromium contents discourage re-crystallization.

Grain boundaries were often decorated with fine non-equiaxed precipitation on the order of 50 nm, but size and distributions varied from one grain boundary to another. Such precipitation is typically produced during furnace cooling following the 1000°C annealing treatment [8].

3.2. Microstructures following irradiation

The major effects of irradiation both at 200°C and at 300°C were development of a fine structure and evidence of an increased internal strain based on lack of Kikuchi band structure. The fine structure was apparent under strain contrast conditions and can be expected to be the cause of the internal strain. Diffraction patterns showed little detail, but evidence for streaking at approximately 2/3 ⟨2 2 2⟩ found previously [9] could be identified easily, whereas streaking at 3/4 ⟨2 0 0⟩ was very faint and usually impossible to see. Images using 2/3 ⟨2 2 2⟩ were very weak, but the scale of the structure matched that found in matrix dark field images approaching weak beam conditions. Therefore, it is apparent that precipitation due to 2/3 ⟨2 2 2⟩ is responsible for the fine structure and the internal strain observed.

3.3. Examples

Examples of these microstructures are provided in Figs. 1 and 2. Fig. 1 gives an example for each of the irradiated conditions at low magnification. The structures appear similar to those found in the unirradiated conditions except that fine precipitates on grain boundaries are no longer visible, and fine structure can be seen within grains. Large precipitate particles, present prior to irradiation, are retained, but the smaller precipitates found on grain boundaries may have become invisible because they are hidden by the fine structure formed during irradiation.

Fig. 2 was prepared to show features of the fine structure within grains at higher magnification. For each irradiation condition, weak beam dark field images for the same area are shown using $g = 0\,1\,1$ and $2\,0\,0$, respectively, for foil conditions near (0 1 1) so that the corresponding g vectors are orthogonal with ⟨2 0 0⟩ horizontal. Where the information was available, the (0 1 1) pattern, with 000 on the lower left, has been inset. Also of note is that under the specimen identification code P224, a precipitate dark field image with $g = \sim 2/3$ [2 2 2] has been inset. From this figure, the following can be demonstrated. Diffraction information indicates only

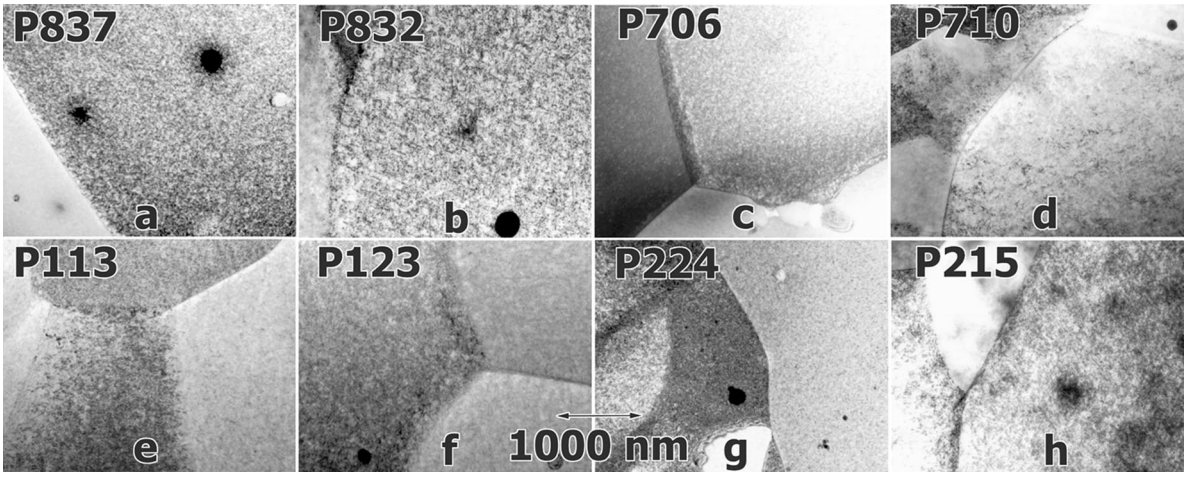

Fig. 1. Low magnification examples of irradiated microstructures in specimens of V–(3–6%)Cr–(3–5%)Ti irradiated in the ATR-A1 experiment showing the large heat 832665 at 200°C and 300°C in (a) and (b), heat T87 at 200°C and 300°C in (c) and (d), heat T91 at 200°C and 300°C in (e) and (f), and heat T92 at 200°C and 300° in (g) and (h).

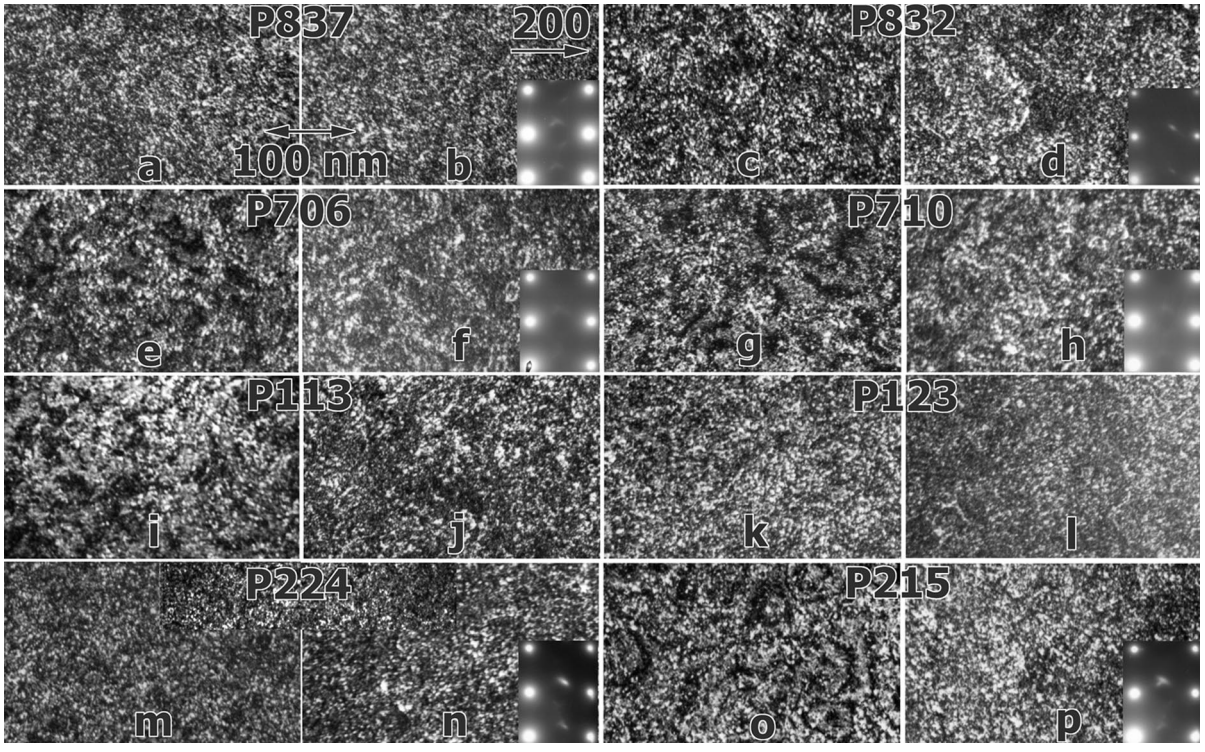

Fig. 2. Dark field images using G = [0 1 1] and [2 0 0], respectively, of irradiated microstructures in specimens of V–(3–6%)Cr–(3–5%)Ti from the ATR-A1 experiment showing the large heat 832665 at 200°C in (a) and (b) and at 300°C in (c) and (d), heat T87 at 200°C in (e) and (f) and 300°C in (g) and (h), heat T91 at 200°C in (i) and (j) and at 300°C in (k) and (l), and heat T92 at 200°C in (m) and (n) and at 300°C in (o) and (p). Where available, (0 1 1) diffraction patterns have been inserted and P224 contains an insert showing precipitate dark field contrast.

the presence of intensity in the vicinity of 2/3 ⟨2 2 2⟩; intensity in the vicinity of ~3/4 ⟨2 0 0⟩ is very weak. Precipitate dark field images formed using $g = 2/3\ \langle 2\,2\,2\rangle$ are very weak, but indicate the presence of very small particles. Similar features can be seen in all other weak beam images indicating that the responsible precipitate

particles provide strain fields visible under strain contrast conditions (or that matrix [2 0 0] and [0 1 1] reflections superimpose on precipitate reflections). Comparison of [2 0 0] and [0 1 1] images consistently shows fine structure in both, but coarser structure in the [2 0 0] images as well. Therefore, this coarser structure corresponds to the dislocation configurations. Fig. 2(f) in particular can be interpreted to indicate the presence of dislocation loops approximately 20 nm in diameter. Insufficient information is available to define the character of the dislocation Burgers vector unambiguously due to complexities arising from the precipitation, but images do correlate with anticipated $a/2\ \langle 1\,1\,1\rangle$ character. Therefore, the dislocation density is significantly lower than the precipitate particle density and the major hardening due to irradiation can be anticipated from the precipitate structure.

3.4. Quantification of precipitation

As all weak beam images presented in Fig. 2 were taken with matching stereo pairs, it is possible to quantify the precipitate features in order to estimate the consequences of such features on mechanical properties. Table 2 provides results from measurements of the fine structure observed on $\langle 0\,1\,1\rangle$ images, assuming the particles are spherical. At least 50 particles were measured for each area of interest, but the values obtained must be considered estimates due to the difficulty of the analysis. Therefore, variations obtained in mean diameter may be statistically insignificant and variations in volume fraction should only be considered as indication of possible trends. Based on examination of stereo information in thin areas, it can be noted that the precipitates are non-uniformly distributed. Precipitation is in patches with areas of similar size separating the patches. The results in Table 2 indicate that precipitates are between 3 and 4 nm in average diameter at number densities between 1 and 3×10^{17} cm^{-3} corresponding to volume fractions on the order of 0.5%. Surprisingly, the observed response appears to be insensitive to the irradiation temperature and the only heat to heat variation that may be significant is the higher number density by a factor of two found for 832665BL-71.

4. Discussion

The purpose of this work is to provide microstructural information allowing interpretation of test results for mechanical properties measurements including those on miniature tensile specimens and disks tested by shear punch procedures [3,4]. Results are not yet available, but preliminary results [10] indicate that all materials showed large degradation in properties following irradiation.

Based on the present and previous microstructural observations [9], mechanical property degradation appears to be due to precipitation during irradiation. Unfortunately, the composition of the precipitate has not yet been established, so that it is not yet possible to provide recommendations for composition modifications for improved properties. However, recent results [11,12] indicate that precipitation of interstitial elements with titanium is likely responsible. This discussion is provided as further speculation on the likely causes for the behavior observed.

It is noteworthy that diffraction response for precipitates formed during irradiation is found to vary with irradiation temperature. Following irradiation at 400°C to 4.5 dpa in HFIR, streaks were found both at 3/4 $\langle 2\,0\,0\rangle$ and 2/3 $\langle 2\,2\,2\rangle$, whereas the present results following irradiation at 200°C and 300°C to 3 or 4 dpa show streaks only at 2/3 $\langle 2\,2\,2\rangle$. Therefore, two types of precipitation formed at 400°C, but at lower temperatures, one of these precipitates is not found, at least following irradiation to doses on the order of 4 dpa. However, the identification of the precipitate composition is still uncertain [11]. Chung et al. [13] have identified features with 2/3 $\langle 2\,2\,2\rangle$streaks as VC, but volume fraction measurements in the present work do not appear to correlate with carbon content. Therefore, identification of the precipitates formed in this V–(3–6%)Cr–(3–5%)Ti during irradiation has not yet been satisfactorily determined.

Table 2
Irradiation induced precipitate size and density as determined from weak beam images

ID	Conditions: heat/dose/temp	Mean diameter (nm)	Number density (10^{17} cm^{-3})	Volume fraction (%)
P837	BL-71/3 dpa/200°C	3.3	3.2	0.6
P832	BL-71/4 dpa/300°C	3.5	2.5	0.6
P706	T87/3 dpa/200°C	3.9	1.6	0.6
P710	T87/4 dpa/300°C	3.6	1.6	0.5
P113	T91/3 dpa/200°C	3.8	1.8	0.6
P123	T91/4 dpa/300°C	3.0	1.1	0.2
P224	T92/3 dpa/200°C	3.9	1.6	0.5
P215	T92/4 dpa/300°C	3.8	2.0	0.7

The precipitation identified following irradiation in the ATR-A1 experiment at 200°C and 300°C is found to consist of particles on the order of 3 nm in diameter at densities in the range $1–3 \times 10^{17}$ cm^{-3} corresponding to volume fractions on the order of 0.5%. As the precipitates are best imaged using strain contrast, it is likely that strain centers of this size and density would have a major effect on hardening and embrittlement. It is not yet understood why precipitation is similar in size following irradiation at both 200°C and 300°C. Nor is it understood why number densities are found to vary as a function of composition such that heat 832665 gave higher densities by about a factor of two. Given the very small sizes of the precipitates, perhaps the best explanation lies in experimental uncertainty. Errors on the order of a factor of two are not unreasonable with such fine microstructures.

5. Conclusions

Eight specimen conditions from the ATR-A1 experiment irradiated at 200°C and 300°C to ~4 dpa, comprising four heats of V–(3–6%)Cr–(3–5%)Ti given similar preirradiation heat treatments and directly corresponding to mechanical properties specimens, have been examined to identify the cause of irradiation hardening. Dislocation loops could be identified but hardening is found to be due to precipitation of a high density of small particles. Precipitation differs from response at 400°C, because one precipitate type dominates at these lower irradiation temperatures. Particle sizes are on the order of 3 nm in diameter at densities in the range $1–3 \times 10^{17}$ cm^{-3} corresponding to volume fractions on the order of 0.5%. The irradiation-induced precipitation appears to be insensitive (to within a factor of ~2) to preirradiation heat treatment and composition.

Acknowledgements

Work supported in part by the US Department of Energy under Contract DE-AC06-76RLO 1830.

References

[1] B.A. Loomis, A.B. Hull, D.L. Smith, J. Nucl. Mater. 179–181 (1992) 148.
[2] S.J. Zinkle, D.J. Alexander, J.P. Robinson, L.L. Snead, A.F. Rowcliffe, L.T. Gibson, W.S. Eatherly, H. Tsai, Fusion Materials Semiannual Progress Report for period ending 31 December 1996, DOE/ER-0313/21, p. 73.
[3] To be reported by S.J. Zinkle et al., ORNL.
[4] M.L. Hamilton et al., these Proceedings, p. 418.
[5] H. Tsai, L.J. Nowicki, M.C. Billone, H.M. Chung, D.L. Smith, Fusion Materials Semiannual Progress Report for period ending 31 December 1997, DOE/ER-0313/23, p. 70.
[6] M.L. Grossbeck, Fusion Materials Semiannual Progress Report for period ending 31 December 1997, DOE/ER-0313/23, p. 157.
[7] H. Tsai, R.V. Strain, I. Gomes, D.L. Smith, Fusion Materials Semiannual Progress Report for period ending 30 June 1997, DOE/ER-0313/22, p. 303.
[8] D.S. Gelles, H. Li, Fusion Materials Semiannual Progress Report for period ending 30 June 1997, DOE/ER-0313/19, p. 22.
[9] D.S. Gelles, H.M. Chung, Fusion Materials Semiannual Progress Report for period ending 30 June 1997, DOE/ER-0313/22, p. 39.
[10] S.J. Zinkle, ORNL, private communication.
[11] D.S. Gelles, P.M. Rice, S.J. Zinkle, H.M. Chung, J. Nucl. Mater. 258–263 (1999) 1380.
[12] S.J. Zinkle, A.F. Rowclliffe, L.L. Snead, D.J. Alexander, in: 19th ASTM Symposium on Effects of Radiation on Materials, 16–18 June 1998, Seattle, WA, unpublished.
[13] H.M. Chung, J. Garza, D.L. Smith, Fusion Materials Semiannual Progress Report for period ending 30 June 1998, DOE/ER-0313/24, p. 49.